

1-1-2007

Extended System Transfer Compensation for Parametric Imaging in Ultrasonic Response Assessment of Anti-Cancer Therapies

Sebastian Brand
University of Halle-Wittenberg

GJ Czarnota
Ryerson University

Michael C. Kolios
Ryerson University, mkolios@ryerson.ca

Follow this and additional works at: <http://digitalcommons.ryerson.ca/physics>

 Part of the [Atomic, Molecular and Optical Physics Commons](#)

Recommended Citation

Brand, Sebastian; Czarnota, GJ; and Kolios, Michael C., "Extended System Transfer Compensation for Parametric Imaging in Ultrasonic Response Assessment of Anti-Cancer Therapies" (2007). *Physics Publications and Research*. Paper 9.
<http://digitalcommons.ryerson.ca/physics/9>

This Conference Presentation is brought to you for free and open access by the Physics at Digital Commons @ Ryerson. It has been accepted for inclusion in Physics Publications and Research by an authorized administrator of Digital Commons @ Ryerson. For more information, please contact bcameron@ryerson.ca.

Extended system transfer compensation for parametric imaging in ultrasonic response assessment of anti-cancer therapies

Sebastian Brand
Q-BAM Group, Orthopedics Dept.
University of Halle-Wittenberg
Halle, Germany
Sebastian.Brand@medizin.uni-halle.de

G.J.Czarnota^{2,3}, M.C.Kolios^{1,3}
¹Physics Department, Ryerson University
²Dept. of Radiation Oncology /
³Dept. of Medical Biophysics
University of Toronto
Toronto/Ontario, Canada

Abstract—The assessment of the tissue response in anti cancer therapy is a time critical process. The early recognition of a failing treatment might allow an adjustment to increase the success rate and spare unnecessary side effects. Today biopsy and nuclear medicine are commonly used procedures for assessing the treatment success. However biopsies are invasive and provide a limited sample volume and nuclear medicine on the other hand requires the application of radioactive agents. It has been observed that ultrasound backscatter properties of cell collections are altered when the cells are respond to an oncological treatment. In previous studies we have estimated spectral properties of ultrasound backscatter using commonly accepted procedures for eliminating system specific transfer properties. These methods proved to be sufficient when investigating regions close to the transducers focus. However, the application in a clinical environment will require the parameter estimation in an extended area combined with parametric imaging. The purpose of this work is to implement more accurate methods for the determination of the effective scatterer size in quantitative high frequency ultrasound. To improve the accuracy but also extend the axial image depth for parametric imaging we developed an algorithm for eliminating the transfer properties of the equipment. It accounts for the distortion of the incident pulse due to the relative defocus position of a time gate and the corresponding alterations in the spectral shape. Two different methods for estimating the transfer properties were applied. One method used the echoes obtained from a plane reflector at 51 positions within the ± 5 mm range around the transducers focus. The second method derived the required compensation function from the signal variation within a pellet of untreated cells. Both, the axial amplitude variation and the alterations of the spectral shape were derived as a function of the defocus position. The slope of the normalized power spectrum, the effective scatterer size and integrated backscatter coefficients were computed from ultrasound backscatter of cervix carcinoma (HeLa) cells after applying the compensation algorithms. Chemotherapy was applied to induce apoptosis in HeLa cells. At 6 time points after treatment cells were harvested and ultrasound backscatter was recorded using a 20MHz ($f\# 2.35$) and a 40MHz ($f\# 3$) transducer. Within the axial -12dB range of the transducer slope differences of up to -1.2 dB/MHz were observed and compensated. Integrated backscatter coefficients increased by over 300% of the initial values. This study contributes towards a non-invasive method for estimating tissue responses in anti-cancer therapy.

Keywords: *quantitative ultrasound; high frequency ultrasound, HeLa, treatment response, transfer characteristic*

I. INTRODUCTION

Ultrasonic imaging is one of the most utilized imaging modalities applied in medical diagnosis. Commonly the envelope of the backscattered ultrasound signals is used for displaying scattering variations within the tissue. In numerous studies characteristic features of measured ultrasound backscatter were estimated and related to the underlying tissue morphology, to provide additional information to the signal envelope. For this purpose researchers applied quantitative ultrasound methods to investigate signal characteristics in relation to tissue pathologies of the kidney (Insana et al. 1991; Lizzi et al. 1983; Worthington et al. 2001), liver (Gertner et al. 1998; Lizzi et al. 1981), prostate (Fleppa et al. 1996; Schmitz et al. 1999) and of the eye (Lizzi et al. 1983). Commonly the system specific transfer properties are accounted for by normalizing the measured power spectra to the pulse reflected from a plain reflector placed at the transducers focus (Lizzi et al. 1983). In previous studies we have shown that integrated backscatter coefficients and effective scatterer size estimates of ensembles of cells alter in correspondence to the exposure to chemo therapy (Brand et al. 2005; Czarnota et al. 1997; Kolios et al. 2002). Chemotherapeutic treatment commonly causes the cell to undergo cell death. During that process a cell initiates a sequence of changes that affect its structure. In apoptotic cell death the chromatin condenses, the nucleus shrinks and the cell fragments into so-called apoptotic bodies. This process causes changes in the cell structure that are potentially detectable with ultrasound. For parametric imaging using spectral parameters of the underlying backscatter signals it is required to extend the physical analysis range to beyond the focal zone of the transducer. However, when leaving the focal region a compensation algorithm for the system dependent transfer properties is needed that exceeds calibrating to a pulse reflected at the transducers focus. Therefore, we estimated properties of the transducer specific diffraction pattern that impact the axial amplitude distribution in combination with the spectral shape of the propagating ultrasound signals. Compensation functions were derived and applied to ultrasound backscatter signals

obtained from HeLa cells that were exposed to chemo therapy for estimating the slope of the normalized power spectra and the effective scatterer size.

II. MATERIALS AND METHODS

A. Cell culture and sample preparation

Human cervix carcinoma cells (HeLa from ATTC) were cultured in minimum essential media (MEM) supplemented with 10% heat inactivated fetal bovine serum containing 0.1% gentamycin in a humidified atmosphere at 37°C containing 5% CO₂. Cells were thawed from frozen stock and cultured in cell culture flasks containing 15ml of the described medium. Apoptosis was induced in HeLa cells by exposure to a concentration of 10µg/ml cisplatin. The treatment duration was 0h, 8h, 12h, 18h, 24h, and 32h respectively. Cells were detached and centrifuged at 216 x g before the medium was removed. Cells were then re-suspended in phosphate buffered saline (PBS) and centrifuged to the final pellet at 1942 x g. Cell pellets had a diameter of 10mm and a height of approximately 2-4mm. During ultrasonic data acquisition cell pellets were submerged in PBS that acted as the coupling medium. Cell pellets were fixed in 10% (w/f) formalin in PBS in preparation for histology.

B. Transfer properties estimated by a plain reflector

For estimating both the axial amplitude distribution and the axial variation of the pulse distortion pulses reflected from a plain reflector were recorded. As a target a flat quartz cylinder (Edmund Industrial Optics Inc., USA, part 43424) with a diameter of 30mm and a thickness of 10mm was used. Pulses reflecting off the plain surface were recorded at 51 positions within the ±5mm range of around the transducers focus. Power spectra of all pulses were computed and normalized to the power spectrum of the focal echo. From that data the axial distribution of the amplitude and the axial distribution of the slope of the normalized power spectra were estimated and an appropriate function for compensating the transfer properties of the used ultrasonic device was derived.

C. Transfer properties estimated from a cell phantom

Target signals scattered from cell ensembles were recorded. Assuming a homogenous scatterer distribution in a pellet containing untreated HeLa cells, native ultrasound backscatter signals were used. The cell pellets had a thickness of approximately 2-4mm. The focal position of the transducer was placed at the centre of the cell pellet. From two separate cell pellets that contained untreated HeLa cells five scan planes containing 80 rf-lines, were recorded from each specimen. To derive the axial distribution of both amplitude and the slope of the normalized power spectrum a sliding window algorithm was applied to the unprocessed rf signals. That algorithm applied a window length of 460 µm (approximately 5 wavelengths) and a separation between two adjacent windows of 45 µm. Using a Gaussian window shape the algorithm provided 80 window positions along each of the 80 rf-signals. Power spectra were computed for each of the

windowed signals. To derive the axial distribution of the amplitude power spectra were averaged along the lateral dimension and the maximum value of each power spectrum was stored. Following all averaged power spectra were normalized to the power spectrum with the maximum amplitude (focus). Linear regression analysis of the normalized power spectra along the axial direction provided a slope value for each window position, representing the pulse distortion.

D. Ultrasonic experiments

Ultrasonic data acquisition was performed using an ultrasound biomicroscope (UBM, VisualSonics Inc., Toronto, Canada) in combination with a 20MHz and 40MHz transducer (VisualSonics Inc., Toronto, Canada). The 20 MHz transducer had a f-number of 2.35, a relative bandwidth of 100% and an aperture diameter of 8.5mm. The specifications of the 40MHz transducer were: f-number 3; relative bandwidth 91%; aperture diameter 3mm. The UBM enabled real time B-mode imaging of the interrogated specimen and acquisition of the unprocessed rf-backscatter signals. The sampling frequency of the UBM's internal AD-converter was 500 MHz. Digitized data were stored on the internal hard drive and were transferred to a desktop computer for offline analysis. Ultrasonic investigations were performed on one cell pellet containing HeLa cells at each time point during the chemotherapeutic treatment. From each cell pellet 80 rf-lines were recorded at five different scan-planes. The length of each rf-line was 2-3 mm and the scan line was centred at the transducers focus, which was consistently placed approximately 2 mm below the pellet surface. To obtain statistically independent data, scan lines were separated by 200 (one beam width) µm. A custom made MATLAB (Mathworks, Natick, USA) program was developed for both derivation of the compensation functions and signal analysis. This software allowed reconstruction of the B-mode images and the selection of a region of interest (ROI) enclosing only signals from inside the cell pellet. ROI's were placed inside the cell pellet and contained 80 rf-lines. For estimating averaged parameter values, 3 ROI's were chosen within each investigated cell pellet. All ROI's were centred vertically at the transducers focus and were approximately 2mm in height. The custom made software applied a sliding window algorithm to each of the 80 rf-lines contained in each ROI, with settings for window length and separation as mentioned above. Windowed signals were then Fourier transformed using the MATLAB signal processing toolbox. According to the relative position between the window and the transducers surface, the diffraction pattern caused amplitude distribution was accounted for, at each distinct window position using the derived compensation function. Power spectra were then normalized to the spectrum of the pulse reflected from the flat quartz cylinder placed at the focus. The axial distribution of the slope of the normalized power spectrum, caused by the diffraction pattern was accounted for by using the corresponding slope compensation function. For each experiment the analysis was performed twice applying each of the two compensation algorithms. For spectroscopic analysis, compensated and normalized power spectra were averaged over all scan lines and window positions. From the resulting normalized power spectrum the

value of the slope and integrated backscatter coefficients were computed. Furthermore from the slope of the normalized power spectrum an estimate of the effective scatterer size was derived using an algorithm proposed by (Lizzi et al. 1983). Integrated backscatter coefficients were estimated using a general computation algorithm described by (Turnbull et al. 1989).

III. RESULTS AND DISCUSSION

A. Compensating transfer properties using calibration functions

Figure 1 (left) shows the axial intensity distribution estimated a) using a flat quartz cylinder as a reflection target and b) backscatter signals from a pellet of untreated HeLa cells. The position "0 mm" corresponds to the radius of curvature (ROC) of the distinct transducer. All curves are normalized to the value at the geometric focus. It can be seen from Fig.1 that the intensities reach maximum values at different positions according to the material the distribution was measured with. For both transducers and both materials (reflector and cell pellet) a formation of a focal region can be recognized that is close to the theoretically expected focus position. The graphs in Fig.1-right display the slope distribution of the normalized power spectra as a function of the axial distance. The value zero at the position "0mm" is due to the normalization to the signal obtained at that position. For reflector measurements a steep drop of the slope values can be seen at approximately 1mm negative defocus. This effect is similar for both transducers used. When estimating the slope of the normalized power spectra from the backscatter obtained from the cell pellets slope values measured with the 20MHz transducer vary in the ± 0.2 dB/MHz range. For the 40MHz transducer these variations are 0.4dB/MHz. It was expected that the distribution of axial intensity and slope values of the normalized power spectra deviate between the two estimation methods. The steeper post focal decrease of the intensity distribution is explained by the attenuation inside the cell

pellet. Whereas the pulse measured with the plain reflector travels through distilled water, the sound pulse transmitted into the cell pellet is additionally attenuated by absorption and scattering, which decreases its signal intensity.

The major difference observed in the values of the slope of the normalized power spectra is the steep drop prior to the focus. Caused by the strong reflectivity of the solid glass reflector additional wave components originated further off from the central axis of the transducer contribute to the pulse formation. Those wave components are not in phase with the on-axis wave components and therefore cause a pulse distortion that is exhibited in the slope values. The larger variations in both intensity and slope estimates obtained from the experiments with the cell pellet at negative defocus positions are explained by the near field structure of the diffraction pattern. Also caused by attenuation is the higher decrease of the slope estimates at positive defocus positions for both transducers. Using a cell pellet allows the estimation of the systems transfer behavior under similar conditions which apply when recording the backscatter signals from a cell pellet during the treatment. Besides the pure transfer properties of the device attenuation in the cell pellet is automatically included in the compensation algorithm and signal changes which are caused by the treatment have a higher impact on the estimated parameter values.

B. Ultrasonic assessment of treatment induced tissue responses

The compensation functions obtained with both methods were applied to estimate spectral parameter values from ultrasound backscatter signals obtained from HeLa cell pellets that have been exposed to chemotherapy. Changes in ultrasound integrated backscatter coefficients as a function of treatment time can be seen in Fig.2. Starting 8h after initiating the treatment values increase from approximately $2E-4$ 1/(sr mm) to $6E-4$ 1/(sr mm) for the 20MHz transducer and to $8E-4$ 1/(sr mm) for the 40MHz transducer. The trends and the values are similar for estimates obtained with both compensation

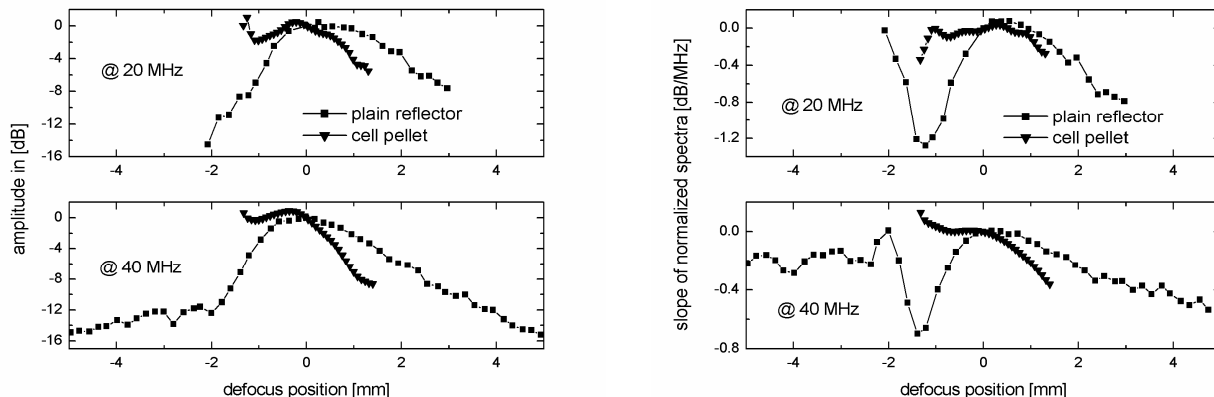


Figure 1: Transfer characteristic of the UBM in combination with a 20MHz and a 40MHz transducer. Left: Axial intensity distribution of signals reflected from a quartz plate vs. signals scattered inside a cell pellet. Right: Axial distribution of the slope of the power spectra normalized to the power spectrum of the pulse received at the transducers focus. Values for both amplitude and normalized slope estimated closest to the transducer surface are assumed to be impacted by the surface of the cell pellet.

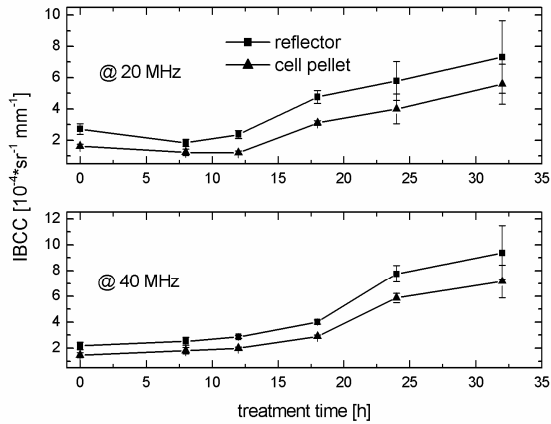


Figure 2: Integrated backscatter coefficients of ultrasound backscatter signals obtain from pellets containing HeLa cells exposed to oncological treatment. Parameters were computed from the signals of both transducers (20MHz and 40MHz).

functions, which was expected considering the similarities of the compensation functions of the intensity distribution.

Table 1 shows values of the spectral slope estimated from a HeLa cell pellet before exposing it to treatment. It should be noted that values between the compensation methods differ, which can be explained by the noticeable differences in the compensation functions before the focus which contribute to the averaged parameter estimates of the spectral slope.

It should also be noted that in the quartz plate compensation as a function of axial depth, only the coupling medium exists between the transducer and reflection plane of interest. In the case of the cell pellet compensation, the coupling medium and a variable portion of the cell pellet medium are in-between the transducer and plane of interest. Whereas this allows for an automatic compensation for attenuation assuming that the attenuation does not change as a function of treatment, the diffraction pattern of the transducer may also be altered. Further experiments are underway to perform the same compensation experiment by keeping the focus slightly below the cell pellet surface and altering the distance between the pellet surface and the transducer (as was done for the quartz plate) and other media that may be more suitable for such corrections (e.g. a water-oil interface).

IV. CONCLUSIONS

In conclusion we have investigated a compensation algorithm derived from native backscatter signals obtained by a material similar to the investigated specimen that may be more appropriate than normalizing to a plain, solid reflector. Normalizing to those signals will emulate the system specific transfer properties under the same sound propagation conditions as in the actual experiment.

ACKNOWLEDGMENTS

The authors acknowledge the financial support of the Whitaker Foundation (grants RG-01-0141), the Natural Sciences and Engineering Research Council (NSERC, CHRP

compensation	20 MHz	40 MHz
cell pellet	0.65 dB/MHz	0.14 dB/MHz
Reflector	1.32 dB/MHz	0.43 dB/MHz

Table 1: Estimated values of normalized spectral slope using compensation functions derived from measurements at a plain reflector and from analysing backscatter from a HeLa cell pellet.

grant 237962-2000) and the Ontario Premier's Research Excellence Awards (PREA 005-0730). The authors also thank Arthur Worthington and Anoja Gilles for technical assistance. The presentation of this work was kindly supported by the GlaxoSmithKline Foundation.

REFERENCES

- [1] Brand, S., Weiss, E. C., Lemor, R. M. and Kolios, M. C. High frequency ultrasound tissue characterization and acoustic microscopy of intracellular changes. *Ultrasound in Medicine and Biology* submitted: 2007; 882-85.
- [2] Czarnota, G. J., Kolios, M. C., Vaziri, H., Benchimol, S., Ottensmeyer, F. P., Sherar, M. D. and Hunt, J. W. Ultrasonic biomicroscopy of viable, dead and apoptotic cells. *Ultrasound in Medicine and Biology* 23(6): 1997; 961-5.
- [3] Feleppa, E. J., Kalisz, A., SokilMelgar, J. B., Lizzi, F. L., Liu, T., Rosado, A. L., Shao, M. C., Fair, W. R., Wang, Y., Cookson, M. S., Reuter, V. E. and Heston, W. D. W. Typing of prostate tissue by ultrasonic spectrum analysis. *Ieee Transactions on Ultrasonics Ferroelectrics and Frequency Control* 43(4): 1996; 609-619.
- [4] Gertner, M. R., Worthington, A. E., Wilson, B. C. and Sherar, M. D. Ultrasound imaging of thermal therapy in in vitro liver. *Ultrasound in Medicine and Biology* 24(7): 1998; 1023-32.
- [5] Insana, M. F., Hall, T. J. and Fishback, J. L. Identifying acoustic scattering sources in normal renal parenchyma from the anisotropy in acoustic properties. *Ultrasound Med Biol* 17(6): 1991; 613-26.
- [6] Kolios, M. C., Czarnota, G. J., Lee, M., Hunt, J. W. and Sherar, M. D. Ultrasonic spectral parameter characterization of apoptosis. *Ultrasound in Medicine and Biology* 28(5): 2002; 589-97.
- [7] Lizzi, F. L., Feleppa, E. J. and Yaremko, M. M. Liver tissue characterization by digital spectrum and cepstrum analysis. *Proceedings of the IEEE Ultrasonics Symposium*: 1981; 575-578.
- [8] Lizzi, F. L., Greenebaum, M., Feleppa, E. J., Elbaum, M. and Coleman, D. J. Theoretical framework for spectrum analysis in ultrasonic tissue characterization. *J Acoust Soc Am* 73(4): 1983; 1366-73.
- [9] Schmitz, G., Ermert, H. and Senge, T. Tissue-characterization of the prostate using radio frequency ultrasonic signals. *IEEE Transactions on Ultrasonics Ferroelectrics and Frequency Control* 46(1): 1999; 126-138.
- [10] Turnbull, D. H., Wilson, S. R., Hine, A. L. and Foster, F. S. Ultrasonic characterization of selected renal tissues. *Ultrasound Med Biol* 15(3): 1989; 241-53.
- [11] Worthington, A. E. and Sherar, M. D. Changes in ultrasound properties of porcine kidney tissue during heating. *Ultrasound Med Biol* 27(5): 2001; 673-82.